3.3. Performance of $SIF_{Fuzzy\text{-}APAR}$

The $SIF_{fuzzy\text{-}APAR}$ modelled data developed through the injection of APAR into the SIF_{fuzzy} under six different combinations (C1-C6) showed a very prominent wide diversity of signals over different vegetation groups as well as over different ecosystems (Figure 9). The $SIF_{fuzzy\text{-}APAR}$ modelled map under C6 (Figure 9A) represents a strong signal over forest and meadows ranging from 0 to 1.34. The peatland area was characterized with complex mixed signals, whereas non-vegetated areas like forest clearings and post-agricultural lands have a very weak signal in the modelled map. Similarly, the $SIF_{fuzzy\text{-}APAR}$ under C2 (Figure 9B), C3 (Figure 9C), and C4 (Figure 9D) also represent the highest consistency of signals over forest and meadows ranging from 0-1.41, 0-1.38, and 0-1.48, respectively. Complex and mixed signals, as well as poor signals of $SIF_{fuzzy\text{-}APAR}$, were observed in peatland and non-vegetated areas in these three modelled maps. The distribution of modelled $SIF_{fuzzy\text{-}APAR}$ signals for C5 and C6 were similar to other $SIF_{fuzzy\text{-}APAR}$ maps and ranged from 0 to 1.46 and from 0 to 1.51, respectively. Similar to SIF_{fuzzy}, intensities of colours for outputs of C3 and C5 models (with the exclusion of PRI and inclusion of EVI) are much lower than the others, indicating lower pixel values for most of the ecosystems. Whereas, intensities and contrasts of colours are much higher for C2, C4, and C6 models with the inclusion of PRI, indicating higher pixel values. Outputs of the C1 model represent a rather moderate strength of signals.

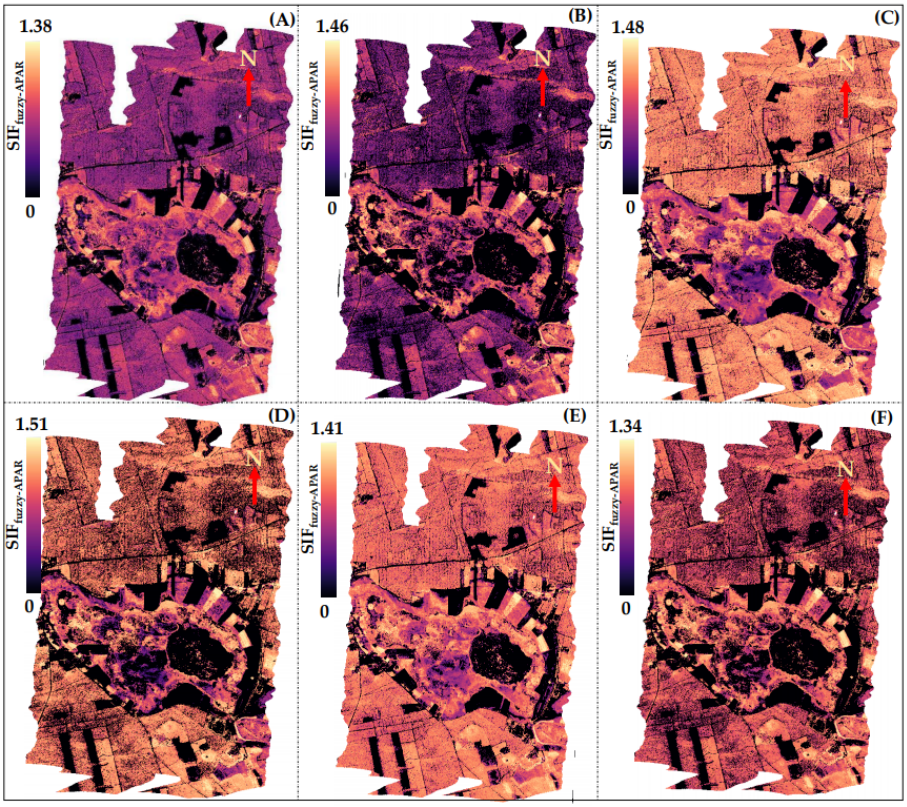

Figure S9. Simulated $SIF_{fuzzy\text{-}APAR}$ maps developed through the injection of APAR into SIF_{fuzzy} for C1-C6 combinations; A) C1 $SIF_{fuzzy\text{-}APAR}$; B) C2 $SIF_{fuzzy\text{-}APAR}$; C) C3 $SIF_{fuzzy\text{-}APAR}$; D) C4 $SIF_{fuzzy\text{-}APAR}$; E) C5 $SIF_{fuzzy\text{-}APAR}$; F) C6 $SIF_{fuzzy\text{-}APAR}$. The colour stretch in the left represents the range of C1-C6 $SIF_{fuzzy\text{-}APAR}$ maps.

We received strong agreement between modelled $SIF_{fuzzy\text{-}APAR}$ and original SIF bands at 760 nm and 687 nm (Table 5). The injection of APAR into SIF_{fuzzy} models has improved the results of simulations for models C6, C1 and C2 and caused the $SIF_{fuzzy\text{-}APAR}$ to correlate stronger for these combinations than SIF_{fuzzy} with the original SIF_{760}. The $SIF_{fuzzy\text{-}APAR}$ model under C1 (*f(NDVI+EVI)*) was identified as the best performing proxy combination for SIF_{760} recorded with the R^2 of 0.56 and the lowest RMSE of 0.195 $mW \cdot m^{-2} \cdot sr^{-1} \, nm^{-1}$ (Table 5). The second-best performing proxy combination for SIF_{760} was $SIF_{fuzzy\text{-}APAR}$ model under C6 (*f(NDVI+EVI+NDVIre+SR+PRI)*) recorded with the R^2 of 0.75 and RMSE of 0.208 $mW \cdot m^{-2} \cdot sr^{-1} \, nm^{-1}$. The $SIF_{fuzzy\text{-}APAR}$ model under C2 determined as *f*(SR+EVI) was recorded with the R^2 of 0.69 and RMSE of 0.229 $mW \cdot m^{-2} \cdot sr^{-1} \, nm^{-1}$. However, the results of models C6 and C2 (Figure 10), as well as PRI-related models of C5, C3, and C4 (Figure 10) tend to

underestimate the SIF for ROIs with the lowest SIF and overestimate for ROIs with the highest SIF.

The injection of APAR into SIF_{fuzzy} models generally has not improved the correlations between $SIF_{fuzzy\text{-}APAR}$ and SIF_{687}. Although recorded with a high R^2 of about 0.9, the RMSE of these regressions was much higher than for SIF_{fuzzy} vs. SIF_{687} (Tables 4 & 5) and the estimated SIF was generally overestimated (Figure 10). The best performing proxy combination for SIF_{687} was $SIF_{fuzzy\text{-}APAR}$ model under C1 (*f(NDVI+EVI))* recorded with the R^2 of 0.89 and the lowest RMSE of 0.143 $mW \cdot m^{-2} \cdot sr^{-1}\ nm^{-1}$. The R^2 and RMSE for regressions between $SIF_{fuzzy\text{-}APAR}$ and SIF_{687} under C6 (*f(NDVI+EVI+NDVIre+SR+PRI))* and C2 *f*(SR+EVI) models were 0.91 and 0.143 $mW \cdot m^{-2} \cdot sr^{-1}\ nm^{-1}$ and 0.87 and 0.144 $mW \cdot m^{-2} \cdot sr^{-1}\ nm^{-1}$, respectively (Table 5).

Table S5. Summary of the statistics (R^2 - coefficient of determination, p-value, SE – standard error, R - correlation coefficient, and RMSE - root mean square error) of linear regressions between $SIF_{fuzzy\text{-}APAR}$ vs. SIF_{760} and $SIF_{fuzzy\text{-}APAR}$ vs. SIF_{687}. The statistical operational outputs were derived based on 19 ROIs representing vegetation groups of the forest, grassland, and peatland.

Combinations	SIF_{fuzzy} functions	R^2	*p*-value	SE	Pearson's r	RMSE $mW \cdot m^{-2} \cdot sr^{-1}\ nm^{-1}$
		$SIF_{fuzzy\text{-}APAR}$ vs. SIF_{760}				
C1	$SIF_{fuzzy\text{-}APAR}$ *(NDVI+EVI)*	0.56	<0.001	0.139	0.75	0.195
C2	$SIF_{fuzzy\text{-}APAR}$ *(SR+EVI)*	0.69	<0.001	0.191	0.89	0.229
C3	$SIF_{fuzzy\text{-}APAR}$ *(NDVI+PRI)*	0.72	<0.001	0.212	0.85	0.269
C4	$SIF_{fuzzy\text{-}APAR}$ *(SR+PRI)*	0.80	<0.001	0.195	0.89	0.254
C5	$SIF_{fuzzy\text{-}APAR}$ *(NDVI+EVI+PRI)*	0.66	<0.001	0.221	0.81	0.256
C6	$SIF_{fuzzy\text{-}APAR}$ *(NDVI+EVI+NDVIre+SR+PRI)*	0.75	<0.001	0.178	0.86	0.208
		$SIF_{fuzzy\text{-}APAR}$ vs. SIF_{687}				
C1	$SIF_{fuzzy\text{-}APAR}$ *(NDVI+EVI)*	0.89	<0.001	0.080	0.95	0.143
C2	$SIF_{fuzzy\text{-}APAR}$ *(SR+EVI)*	0.87	<0.001	0.122	0.93	0.144
C3	$SIF_{fuzzy\text{-}APAR}$ *(NDVI+PRI)*	0.92	<0.001	0.108	0.96	0.327
C4	$SIF_{fuzzy\text{-}APAR}$ *(SR+PRI)*	0.89	<0.001	0.141	0.94	0.266
C5	$SIF_{fuzzy\text{-}APAR}$ *(NDVI+EVI+PRI)*	0.94	<0.001	0.093	0.97	0.305
C6	$SIF_{fuzzy\text{-}APAR}$ *(NDVI+EVI+NDVIre+SR+PRI)*	0.91	<0.001	0.102	0.95	0.154

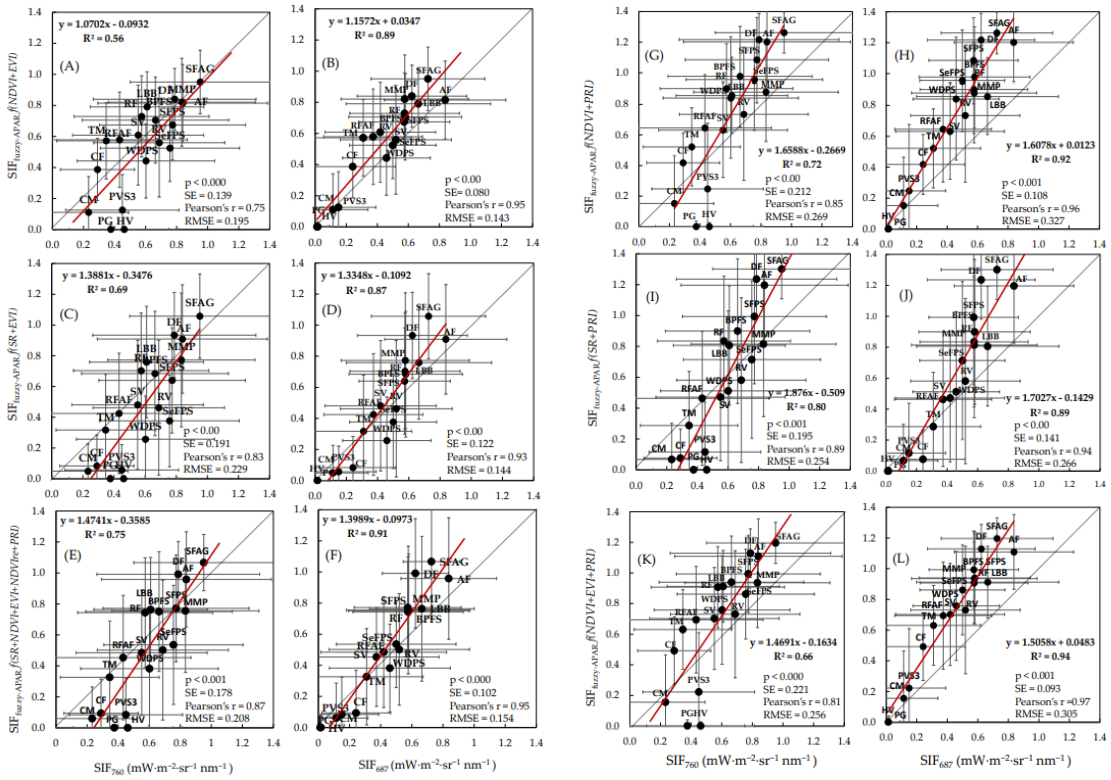

Figure S10. Scatterplots of the fuzzy model outputs ($SIF_{fuzzy\text{-}APAR}$) and original SIFs (SIF_{760} and SIF_{687}) were determined based on *HyPlant* airborne data. A & B – $SIF_{fuzzy\text{-}APAR}$ as expressed by *f(NDVI+EVI)* under model C1; C & D - $SIF_{fuzzy\text{-}APAR}$ as expressed by *f(SR+EVI)* under model C2; E & F - $SIF_{fuzzy\text{-}APAR}$ as expressed by *f(NDVI+EVI+NDVIre+SR+PRI)* under model C6; G & H – $SIF_{fuzzy\text{-}APAR}$ as expressed by *f(NDVI+PRI)* under model C3; I & J – $SIF_{fuzzy\text{-}APAR}$ as expressed by *f(SR+PRI)* under model C4; K & L – $SIF_{fuzzy\text{-}APAR}$ as expressed by *f(NDVI+EVI+PRI)* under model C5. Standard deviations are represented in error bars. The letter abbreviations correspond to the codes of vegetation groups presented in figure 2.

The C1 and C2 related $SIF_{fuzzy\text{-}APAR}$ simulations, based just on two SVIs representing greenness of the canopies and their biomass, can efficiently approximate the original SIF signals at both oxygen absorption bands with the lowest RMSE. Similar to SIF_{fuzzy}, $SIF_{fuzzy\text{-}APAR}$ also showed that the modelled values for these model combinations were very reasonable in correspondence to the original SIF and represented well the signal diversity from the vegetation groups (Figure 11).

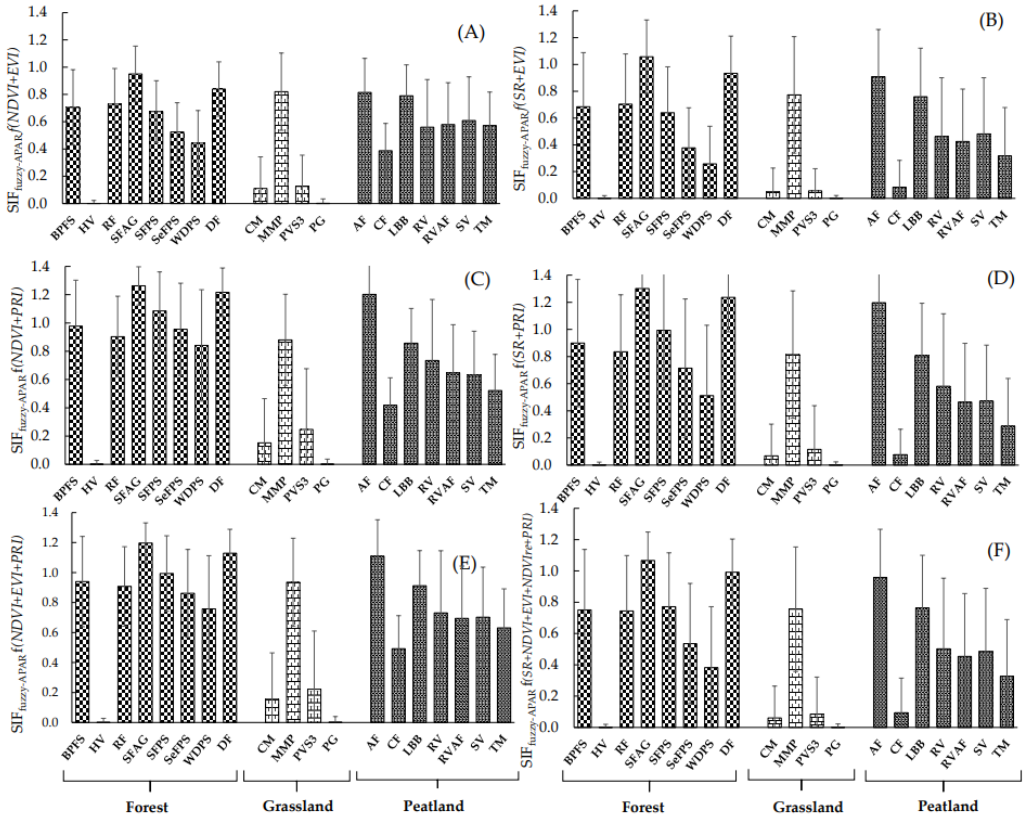

Figure S11. Bar diagrams represent the $SIF_{fuzzy\text{-}APAR}$ values obtained from 19 ROIs. A) $SIF_{fuzzy\text{-}APAR}$ *(NDVI+EVI)* under C1; B) $SIF_{fuzzy\text{-}APAR}$ *(SR+EVI)* under C2; C) $SIF_{fuzzy\text{-}APAR}$ *(NDVI+PRI)* under C3; D) $SIF_{fuzzy\text{-}APAR}$ *(SR+PRI)* under C4; E) $SIF_{fuzzy\text{-}APAR}$ *(NDVI+EVI+PRI)* under C5; $SIF_{fuzzy\text{-}APAR}$ *(SR+NDVI+EVI+NDVIre+PRI)* under C6. Error bars represent the standard deviations.

SFAG, DF, SFPS, BPFS under forest ecosystem, MMP within grasslands, and AF, LBB within peatland were characterized with the highest value of the modelled $SIF_{fuzzy\text{-}APAR}$ signals. The WDPS within the forest ecosystem and RV, RVAF, SV, TM within the peatland ecosystem were estimated with a moderate value of $SIF_{fuzz\text{-}APAR}$ signals in the modelled data. Due to less vegetation cover or absence of vegetation, HV (from the forest), CM, PVS3, PG (from grassland), and CF (from peatland) were characterized with weak concentration from modelled $SIF_{fuzzy\text{-}APAR}$.